Efficient population transfer in a multi-level system using diverging laser beams

A. T. Nguyen[a,*], G. D. Chern[a], D. Budker[a,b], and M. Zolotorev[c]
[a] *Department of Physics, University of California, Berkeley, CA 94720-7300*
[b] *Nuclear Science Division, Lawrence Berkeley National Laboratory, Berkeley CA 94720*
[c] *Center for Beam Physics, Lawrence Berkeley National Laboratory, Berkeley CA 94720*
(July 23, 2000)

We investigate a three-step population scheme to efficiently transfer atoms to a particular metastable state of atomic dysprosium, and present evidence of adiabatic passage in the first step. This scheme will be employed in an ongoing search for parity nonconservation (PNC) in dysprosium. In order to excite a large fraction of the transverse velocity distribution, laser beams with divergences matched to the atomic beam are applied in the first and second step. The total efficiency of the population transfer is analyzed and the implications for the PNC work are discussed.

PACS. 32.80.Qk, 32.80.Ys

I. INTRODUCTION

Recently we conducted a search [1] for atomic parity nonconservation (PNC) in a pair of nearly-degenerate opposite parity states in atomic dysprosium (Dy) (relevant spectroscopic properties have been investigated in Ref. [2]). In addition to the Z^3 enhancement [3] of PNC effects in neutral heavy atoms (where Z is the atomic number), this search was motivated by theoretical estimates [4] predicting a substantial enhancement due to the small energy separation of the opposite parity levels. Unfortunately, despite the fact that the experimental sensitivity to the PNC matrix element (H_w) considerably exceeds that of all other PNC experiments performed to date (see, e.g., Ref. [5] for a review), no PNC effect was detected, and an upper limit of $|H_w| < 5$ Hz (68% C.L.) was established.

This statistics-limited experiment used pulsed lasers with repetition rate of 10 Hz, which led to a low effective duty cycle ($\sim 10^{-4}$). Thus, the goal of the current work is to increase the counting rate by developing an efficient population method of the nearly-degenerate states using cw lasers [6]. Using this method we plan to perform a PNC measurement with significantly improved sensitivity. A detailed discussion of the motivation for such a measurement was given in Refs. [1,6].

In the PNC experiment, we use a weakly collimated atomic beam which has a transverse Doppler width $\sim$ 100 MHz. Thus, light from a collimated, narrow-band cw laser only interacts with a small fraction of the transverse velocity distribution. One method to increase the fraction of atoms with which light interacts would be to broaden the laser spectrum, e.g. using an electro-optic modulator. Another solution relies upon a laser beam with a divergence matching that of the atomic beam. In this situation, atoms experience a frequency chirp across resonance as they pass through the laser beam (Fig. 1). Furthermore, for sufficiently large light intensities, this leads to an efficient and robust population inversion analogous to adiabatic passage used in magnetic resonance [7]. Adiabatic passage for optical transitions (for a review see e.g. Ref. [8]) has been previously implemented either by sweeping the transition frequency via the DC Stark effect [9] or by directly changing the light frequency [10]. Diverging laser beams have also been used [11–14], but only to interact with well-collimated atomic or molecular beams (collimation ratio much less than 1:10).

II. POPULATION TECHNIQUE

Three transitions are required to reach the long-lived (> 200 μs) odd parity state of interest (B) in the current population scheme (Fig. 2). In the first transition, 833-nm light excites atoms from the ground state G to state e. 669-nm light is then used to connect state e to the high lying state f. The final step involves spontaneous decay from state f to B at 1397 nm, with a measured branching ratio of .30(9) [6]. The lifetimes of states e and f [6] are 16.5(2.6) μs and 432(5) ns, respectively.

A. Collimated Laser Beam

Consider the interaction of two-level atoms with collimated light, i.e. light whose divergence is much less than that of the atomic beam. Let Γ_0 be the upper state decay rate back to the ground state. By solving the steady-state rate equations, the fraction of atoms, n_2, in the excited state can be found to be (see e.g. Ref. [15]):

$$n_2 = \frac{1}{2}\left(\frac{\kappa}{1+\kappa}\right), \tag{1}$$

where κ is the frequency-dependent saturation parameter,

$$\kappa = \frac{P}{P_s} = \frac{(dE)^2}{2}\left(\frac{\Gamma_0+\Gamma_L}{\Gamma_0+\Gamma_t}\right)\frac{1}{\Delta^2+(\Gamma_0+\Gamma_L)^2/4}. \tag{2}$$

Here P is the time-averaged light power, E is the corresponding electric field amplitude, P_s is the saturation power; d is the transition dipole matrix element, Γ_L is

the laser line width, Γ_t is the reciprocal of the transit time across the light beam, and Δ is the frequency detuning. Here and throughout, $\hbar \equiv 1$. In the high light power limit, $n_2 \to 1/2$.

For a laser beam propagating perpendicular to the atomic beam axis, due to the Doppler effect, the detuning a particular atom sees depends upon its transverse velocity component. To account for this, one takes the convolution of n_2 with the transverse velocity distribution. If this distribution is assumed to be a normalized Gaussian, $D(v)$:

$$D(v)dv = \frac{1}{v_0\sqrt{\pi}} e^{-v^2/v_0^2} dv, \tag{3}$$

where v_0 is some characteristic transverse velocity, then the overall fraction of excited atoms can be approximated by:

$$\tilde{n}_2 = n_2(\kappa_0)\frac{\Gamma'}{\Gamma_D}\frac{\sqrt{\pi}}{2}\, e^{-\Delta^2/\Gamma_D^2}, \tag{4}$$

$$= \frac{1}{2}\frac{\kappa_0}{\sqrt{1+\kappa_0}}\left(\frac{\Gamma_0+\Gamma_L}{\Gamma_D}\right)\frac{\sqrt{\pi}}{2}\, e^{-\Delta^2/\Gamma_D^2}, \tag{5}$$

for $\Gamma' \ll \Gamma_D$. Here κ_0 is the saturation parameter on resonance, $\Gamma' = (\Gamma_0+\Gamma_L)\sqrt{1+\kappa_0}$ is the power broadened line width, and $\Gamma_D = kv_0$ is the Doppler width (k is the wavenumber). Note that the Doppler width defined as the full-width at half-maximum is also often used in the literature: Γ_D (FWHM)$= 2\sqrt{\ln 2}\,\Gamma_D$. For small divergences ($\phi \ll 1$), $v_0 \approx v_p\ \phi/2$ where v_p is the most probable velocity of the atomic beam.

B. Diverging Laser Beam

The situation is quite different for a diverging laser beam. If the divergence is larger than that of the atomic beam, each atom will experience a sweep in light detuning Δ (Fig. 1) and, thus, almost all atoms will encounter resonant light at some point as they pass through the laser beam. Assuming for now, that the excited state lifetime is infinite, adiabatic passage occurs if the electric field amplitude E of the light satisfies the following criterion [16]:

$$\xi = \left|\frac{\dot{\Omega}\Delta - \Omega\dot{\Delta}}{\widetilde{\Omega}^3}\right| \ll 1, \tag{6}$$

where $\Omega = dE$ and $\widetilde{\Omega} = \sqrt{\Omega^2+\Delta^2}$.

In our experiment, we use a cylindrical lens to diverge the beam in the direction along the atomic beam axis (y-axis; see Fig. 1). The electric field for such a beam (with a waist at $x = 0$ and propagating along the x-direction) is given by (see, e.g., Ref. [17]):

$$\mathcal{E}(x,y,t) = E(x,y)\cos(kx - \omega t + \Phi(x,y)), \tag{7}$$

$$\text{where } E(x,y) = E_0\sqrt{\frac{w_0}{w(x)}}e^{-y^2/2w(x)^2}. \tag{8}$$

Here E_0 is the amplitude at the origin, $w(x)$ is the spot size [18], w_0 is the spot size at the waist, and $\Phi(x,y)$ is a position dependent phase. These quantities are related to the Rayleigh range $x_0 = kw_0^2/2$, the far-field full-divergence angle θ, and the radius of curvature $R(x) = x + x_0^2/x$ through the following expressions:

$$w_0 = \frac{2}{k\tan(\theta/2)}, \tag{9}$$

$$w(x) = w_0\sqrt{1+(x/x_0)^2}, \tag{10}$$

$$\Phi(x,y) = k\frac{y^2}{2R(x)} - \frac{1}{2}\tan^{-1}\left(\frac{x}{x_0}\right). \tag{11}$$

Let an atom, traveling in the y-direction with a velocity v, intersect the laser beam axis at $x = a$ ($\gg x_0$) and $t = 0$. For light tuned to the transition frequency, the atom experiences a frequency detuning given by:

$$\Delta(t) = -\frac{d\Phi}{dt} \approx -\frac{kv^2t}{a}. \tag{12}$$

One can verify that for this geometry, ξ (Eq. 6) is maximal at the center of the beam ($t = 0$). Thus, for matched divergences ($\theta \approx \phi$):

$$\begin{aligned}\xi_{max} &= \left|\frac{\dot{\Delta}}{\Omega^2(t=0)}\right| \approx \frac{kv^2/a}{(dE)^2} = 2\frac{\Gamma_D\Gamma_t}{(dE)^2} \\ &= 2\frac{\Gamma_D\Gamma_t}{(dE_0\sqrt{w_0/w})^2} \approx 2\frac{\Gamma_D\Gamma_t}{(dE_0\sqrt{8/ka\theta^2})^2} \\ &= 2\frac{\Gamma_D\Gamma_t}{(2dE_0\sqrt{\Gamma_t/\Gamma_D})^2} = \frac{1}{2}\left(\frac{\Gamma_D}{dE_0}\right)^2,\end{aligned} \tag{13}$$

where $1/\Gamma_t = a\theta/v$ is the the transit time through the atomic beam. Notice that, as a consequence of using a cylindrical lens, this expression does not depend upon a. The power needed to satisfy the adiabatic criterion can be estimated by setting $\xi_{max} = 1$. For example, about 30 mW of 833-nm light is required if we take typical parameters for $d = .1$ MHz/V/cm, $v = 5\times10^4$ cm/s, $\theta = .13$ rad, and $H = .3$ cm for the beam height. These estimates are confirmed by numerical density matrix calculations [24] and experimental observations described below.

The finite lifetime of the excited state imposes an additional constraint upon adiabatic passage: the lifetime τ must be longer than the time T that it takes for the inversion process to occur [7]:

$$T = \left|\frac{\Omega(t=0)}{\dot{\Delta}}\right| \approx \frac{dE}{2\Gamma_D\Gamma_t} \ll \frac{1}{\Gamma_0} \tag{14}$$

$$\to \left(\frac{dE_0}{\Gamma_D}\right)^2\frac{\Gamma_0^2}{\Gamma_D\Gamma_t} \ll 1. \tag{15}$$

This constraint does depend upon a (through Γ_t) and sets an upper limit on the laser power. Using the parameters above and $a = 1$ cm, the time $T \approx .1$ μs, which is much less than the 16 μs lifetime of state e.

C. Magnetic Sublevels

Although each level considered in this population scheme has many magnetic sublevels, the adiabatic passage process can be simplified to the two-level analysis described earlier. To see this, it is convenient to consider a basis $|Jm\rangle$ in which the direction of linear light polarization is taken as the quantization axis. In this basis, light only couples sublevels with the same m. As a result, one has a set of two-level systems in which adiabatic passage occurs independently. For each of the two-level systems there may be different adiabatic criteria, depending upon the dipole matrix element connecting the two sublevels:

$$\langle J'm|d|Jm\rangle = \frac{\langle Jm10|J'm\rangle}{\sqrt{2J'+1}}\langle J'\|d\|J\rangle, \qquad (16)$$

where $\langle Jm10|J'm\rangle$ denotes the appropriate Clebsch-Gordan coefficient and $\langle J'\|d\|J\rangle$ is the reduced dipole matrix element.

D. Overlapping Laser Beams

For a three-level system, efficient population of the target level was demonstrated employing two collimated and partially overlapping laser beams selected to excite two adjacent transitions [19–22]. Full population of this level occurs when an atom first encounters the laser beam needed to excite the second transition. Such a light pulse sequence has been called "counterintuitive." Using the dressed-atom picture, this process can be explained using arguments similar to the case of two-level adiabatic passage [23], but in this case the mechanism relies upon changing light intensities rather than a frequency sweep. Thus we do not employ the "counterintuitive" pulse sequence in this work.

III. EXPERIMENTAL SETUP

Fig. 3 shows the experimental setup. Two cylindrical lenses, with focal lengths 1.27 cm and 10.0 cm, were used for each of the 833- and 669-nm beams. They were mounted on translation stages, allowing the distance between the two light beam axes to be easily varied. Independent control of divergences and focal positions for both lens systems was achieved by moving the lenses along rigid tracks. These parameters were calibrated prior to the experiment with a beam profiler placed at the main laser-atomic beam interaction region. The two beams perpendicularly intersected the atomic beam axis and fluorescence was detected by a photomultiplier tube (PMT). A spherical mirror, placed opposite to the PMT, was used to improve detection efficiency. The 833-nm laser beam was chopped at 500 Hz and the fluorescence signal was detected via a lock-in technique.

A. Atomic Beam

A detailed description of the atomic beam source was given in [1]. Briefly, the oven operated at about 1500 K and produced an atomic beam with a density in the laser-atomic beam interaction region of $\sim 10^{10}$ atoms/cm^3. In order to maintain this high density over the interaction volume with a large transverse dimension (1.5 cm), the oven multislit nozzle array and the external collimators were designed to provide only weak collimation. The measured transverse Doppler width was ~ 65 MHz (FWHM) for the 833-nm transition. This corresponds to a characteristic transverse velocity of 2.7×10^3 cm/s and, thus, a corresponding divergence angle of $\sim .11$ rad.

B. Lasers

Approximately 80 mW of 833-nm light was generated by a single-frequency diode laser (Sanyo DL8032) with an external cavity in the Littrow configuration. A fraction of the light output was sent to a wavemeter and a Fabry-Perot interferometer to monitor the output frequency spectrum. Another portion of the light was sent to an auxiliary laser-atomic beam interaction region (not shown in Fig. 3) located ~ 20 cm downstream from the main interaction region. Here the fluorescence signal from a second PMT was used in a feedback loop to lock the laser on resonance. The power at 833-nm available in the main interaction region was ≈ 65 mW. The laser beam had an elliptical cross section with dimensions of $.2 \times .3$ cm^2 ($1/e^2$ level).

To produce 669-nm light, we used a Coherent 599 dye laser with DCM dye pumped by a 5 W Ar ion laser. Typical stable output powers were ~ 100 mW. Although the laser was locked to a reference cavity, it suffered from frequency instabilities, which effectively broadened the laser line width from the specified < 1 MHz to ≈ 8 MHz. Using an iodine absorption cell, the 669-nm transition was referenced to lines in the vicinity of the $(\nu = 6, \mathcal{J} = 15) \rightarrow (\nu = 4, \mathcal{J} = 14)$ transition connecting the ground $(X^1\Sigma_g^+)$ and first excited $(B^3\Pi_{ou}^+)$ state of I_2 [27], where ν is the vibrational and $\mathcal{J}$ is the rotational quantum number. The light power in the interaction region was ≈ 35 mW. The beam was circular with a diameter of .2 cm ($1/e^2$ level).

IV. RESULTS AND ANALYSIS

A. G → e (833-nm) Transition

We chose the ^{164}Dy line for this investigation because of its large natural isotopic abundance (28.2%) and the fact that it is relatively well-resolved in the 833-nm transition spectrum [6,25]. State e mostly decays back to the ground state with a lifetime of 16.5(2.6) μs. From this,

the reduced dipole matrix element was estimated to be $\langle e\|d\|G\rangle = .55(4)$ ea$_0$.

Fluorescence at 833 nm was recorded as the 833-nm laser frequency was scanned across resonance. Both collimated and diverging 833-nm light were used. Fig. 4 shows peak fluorescence as a function of light power for the two cases. A fit of the collimated beam data to a function of the form given in Eq. (5) yields an effective saturation power of $P_0 \sim .3$ mW. Using a dipole matrix element averaged over the Zeeman sublevels [26] the laser line width was determined to be 2.0(5) MHz. Finally, the fraction of atoms in state e, for 65 mW of collimated light, was found to be 15(5)%.

We diverged the laser beam by putting in the lenses. The light power reaching the interaction region decreased to 50 mW due to reflections off the lens surfaces. The divergence was .06 rad (FWHM) and the atomic beam crossed the laser beam at 1 cm from the focal spot. With the lenses, the peak signal increased by about a factor of 5, which means that the fraction of atoms transferred into state e was $> 50\%$.

We further investigated this transition by using the 669-nm transition to probe the population of atoms in state e. Collimated, low-power (~ 5 mW, $\kappa_0 = .5$) 669-nm light interacted with atoms .1 cm downstream from the 833-nm beam, whose frequency was locked on resonance. The 669-nm light frequency was scanned and fluorescence from state f in the 743-nm channel was detected (see Fig. 2).

The peak fluorescence approximately doubles with the introduction of the diverging laser beam. This is a clear signature of adiabatic passage for atoms near the center of the transverse velocity distribution. The overall fraction of atoms excited to state e is 50(20)%, which is limited by the fact that atoms at the periphery of the transverse velocity distribution are excited less efficiently: the adiabatic criterion (Eq. (6)) is not fully satisfied for atoms moving with large angles with respect to the beam axis since they go through resonance where the light intensity is not maximal.

Fig. 6 shows the 743-nm peak fluorescence as a function of 833-nm light power. It clearly indicates that we are currently limited by the 833-nm light power and suggests that one would need to increase the 833-nm light power by a factor of 2 (~ 100 mW) in order to efficiently excite atoms in all transverse velocity components.

B. e → f (669-nm) Transition

Although the 669-nm laser beam was also made to diverge, conditions for adiabatic passage are not fully satisfied because the lifetime of state f (432(5) ns) is comparable to the inversion time ($T \approx 100$ ns; see expression (15)). Nevertheless, state B is still efficiently populated because atoms, once excited to f, decay to B with high probability (the branching ratio from state f to B is 30(9)%).

Fig. 7 shows 743-nm peak fluorescence with lenses in both beams as a function of the divergence angle of the 669-nm beam. This signal is proportional to the fraction of atoms excited from state e to f. The maximum of the curve is a factor of $\sim$2 larger than for the case of zero divergence (without lenses). To understand this increase, we must consider the widths of the excited distributions for each case. For the case without lenses, the width of atoms excited is determined by the power broadened linewidth of the 669-nm transition ($\sim$ 20 MHz (FWHM)). With lenses, the 669-nm transition excites all of the atoms that had been excited by the 833-nm light. The corresponding width is $\sim$ 40 MHz (FWHM) (see Fig. 5). Thus, the factor of $\sim$ 2 increase in the signal is due only to the ratio of these two widths. Using appropriate steady-state rate equations, the fraction of atoms excited from state e to state f, without lenses, was found to be $> 40\%$. Thus, with lenses, this fraction becomes $> 80\%$.

If we had enough 833-nm power to excite the entire transverse Doppler distribution in the first step, as one can see from the signal decrease (Fig. 7) for 669-nm beam divergences $> .05$ rad (FWHM), a factor of 2-3 more 669-nm power would be necessary to maintain high second step excitation efficiency for all atoms.

V. DISCUSSION

A method of efficient population of state B, the odd parity state of interest for a PNC search in atomic dysprosium, has been developed. This method uses diverging cw laser beams to achieve population transfer over a large fraction of the transverse atomic velocity distribution. The overall population efficiency of state B is $\sim 12\%$ found by multiplying together the efficiencies in all three transitions: 50% for the 833-nm transition, 80% for the 669-nm transition, and 30% for the spontaneous decay branching ratio from state f to state B. For the 833-nm transition, a substantial portion of the transverse velocity distribution underwent adiabatic passage. Further improvements are possible by increasing the power of the lasers used and by utilizing a laser at 1397-nm to induce the f → B transition.

The achieved population efficiency translates into $\sim 10^3$ times higher counting rate compared to the pulsed PNC experiment [1]. With a similar technique and a total integration time of 20 hours, this should allow us to reach a statistical sensitivity to the weak matrix element of $\sim$10 mHz. Somewhat different schemes for a PNC measurement, which take advantage of the finite width of the states, have been recently considered theoretically in Ref. [29].

As a final note, we point out that the unique physical situation available in dysprosium: a pair of long-lived states of opposite parity, whose separation can be

arbitrarily adjusted by applying a small magnetic field, can also be used in a variety of applications beyond the PNC work. As demonstrated in the present work, these levels can be efficiently populated by cw lasers. One particular example, is the possibility of achieving electromagnetically-induced transparency (EIT) [30] in a dc-electric field. EIT in adjacent radio-frequency transitions (which can be used to obtain an order of magnitude narrower rf line widths than those in Ref. [2]) could also be possible.

ACKNOWLEDGEMENTS

We would like to thank D. Weiss for drawing our attention to the use of diverging laser beams. We are grateful to D. F. Kimball and D. E. Brown for many helpful discussions. This research has been supported by UC Berkeley start-up funds, and by an REU supplement to NSF CAREER grant PHY-9733479.

---

* e-mail: atn@socrates.Berkeley.edu

[1] A. T. Nguyen, D. Budker, D. DeMille, and M. Zolotorev, Phys. Rev. A **56**, 3453 (1997).

[2] D. Budker, D. DeMille, E. D. Commins, and M. Zolotorev, Phys. Rev. A **50**, 132 (1994).

[3] M. A. Bouchiat and C. Bouchiat, J. Phys. **35**, 899 (1974).

[4] V. A. Dzuba, V. V. Flambaum, and M. G. Kozlov, Phys. Rev. A **50**, 3812 (1994).

[5] D. Budker, in *Physics Beyond the Standard Model*, Proceedings of the Fifth International WEIN Symposium, P. Herczeg, C. M. Hoffman, and H. V. Klapdor-Kleingrothaus, eds. World Scientific, 1999.

[6] A. T. Nguyen, D. E. Brown, D. Budker, D. DeMille, D. F. Kimball, and M. Zolotorev, in: *Parity Violation in Atoms and Polarized Electron Scattering*, B. Frois and M. A. Bouchiat, eds. World Scientific 457, pp. 295-311 (1999).

[7] A. Abragam, *Principles of Nuclear Magnetism*, (Oxford Univ. Press, Oxford, 1961).

[8] R. B. Vrijen, G. M. Lankhuijzen, D. J. Maas, and L. D. Noordam, Comments At. Mol. Phys. **33**, 67 (1996).

[9] M. Loy, Phys. Rev. Lett. **32**, 814 (1974).

[10] J. S. Melinger, A. Hariharan, S. R. Gandhi, and W. S. Warren, J. Chem. Phys. **95**, 2210 (1991).

[11] S. Avrillier, J.-M. Raimond, Ch. J. Borde, D. Bassi, and G. Scoles, Optics Comm. **39**, 311 (1981).

[12] J. P. C. Kroon, H. A. J. Senhorst, H. C. W. Beijerinck, B. J. Verhaar, and N. F. Verster, Phys. Rev. A **31**, 3724 (1985).

[13] C. Liedenbaum, S. Stolte, and J. Reuss, Physics Reports **178**, 1 (1988).

[14] C. Ekstrom, C. Kurtsiefer, D. Voigt, O. Dross, T. Pfau, and J. Mlynek, Optics Comm. **123**, 505 (1996).

[15] W. Demtroder, *Laser Spectroscopy* (Springer-Verlag, New York, 1996), pp. 90-95.

[16] This adiabatic criterion can be derived in several ways, including the consideration of the Bloch vector model (see e.g. L. Allen and J. H. Eberly, *Optical Resonance and Two-Level Atoms* (Dover, New York, 1975), p. 72.), as well as, the dressed-atom approach (see e.g. B. Shore, *The Theory of Coherent Atomic Excitation, Vol. 1* (John Wiley & Sons, New York, 1990), pp. 220-222.)

[17] A. E. Siegman, *Lasers* (University Science Books, Mill Valley, 1986), Ch. 16.

[18] Note that this definition of w differs from that in Ref. [17] by a factor of $\sqrt{2}$, i.e. it is the half-width measured at the $1/e$ level in power.

[19] U. Gaubatz, P. Rudecki, S. Schiemann, and K. Bergmann, J. Chem. Phys. **92**, 5363 (1990).

[20] M. W. Weitz, B. C. Young, and S. Chu, Phys. Rev. Lett. **73**, 2563 (1994).

[21] B. W. Shore, J. Martin, M. P. Fewell, and K. Bergmann, Phys. Rev. A **52**, 566 (1995).

[22] I. R. Sola, V. S. Malinovsky, B. Y. Chang, et. al., Phys. Rev. A **59**, 4494 (1999).

[23] K. Bergmann, H. Theuer, and B. W. Shore, Reviews of Modern Physics **70**, 1003 (1998).

[24] Numerical calculations were performed utilizing the Liouville equation which describes the evolution of the density matrix ρ with the Hamiltonian H:

$$\frac{d\rho}{dt} = i[\rho, H] - \frac{1}{2}\{\Gamma, \rho\}, \tag{17}$$

where Γ is the relaxation matrix. After the addition of appropriate repopulation terms and application of the rotating wave approximation to H, these equations were numerically integrated. Because this calculation did not take into account the longitudinal velocity distribution and laser line widths, the results were only used to confirm qualitative behavior observed in the experiments. For further details, see the undergraduate thesis of G. D. Chern: http://phylabs.berkeley.edu/budker/.

[25] R. J. Lipert and S. C. Lee, Appl. Phys. B **57**, 373 (1973).

[26] In the presence of the laboratory magnetic field ($\sim .5$ G), the sublevels sufficiently mix within the time of transit through the collimated beam (the g-factors of G and e are 1.24 and 1.28, respectively). Thus, an average over the magnetic sublevels was taken. Averaging is unnecessary for adiabatic passage, since the mixing time (the reciprocal of the Larmor frequency) is longer than the time required for adiabatic inversion.

[27] S. Gerstenkorn and P. Luc, *Atlas du Spectre D'Absorption de la Molecule D'Iode* (Centre National de la Recherche Scientifique, Paris, 1978).

[28] I. I. Sobelman, *Atomic Spectra and Radiative Transitions* (Springer-Verlag, New York, 1992), p. 207.

[29] T. Gasenzer and O. Nachtmann, Los Alamos National Laboratory e-print server document number: hep-ph/9909358, to appear in Eur. Phys. J. D.

[30] S. E. Harris, Physics Today **50**, 36 (1997).

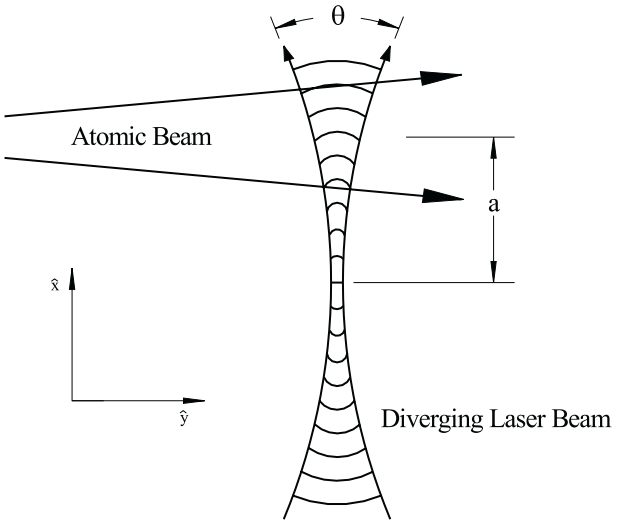

FIG. 1. Atomic beam intersecting a diverging laser beam, with divergence θ. R is the distance from the laser beam waist to the axis of the atomic beam. As atoms traverse the laser beam, they see a frequency sweep in laser detuning which, for sufficient light power, leads to adiabatic passage.

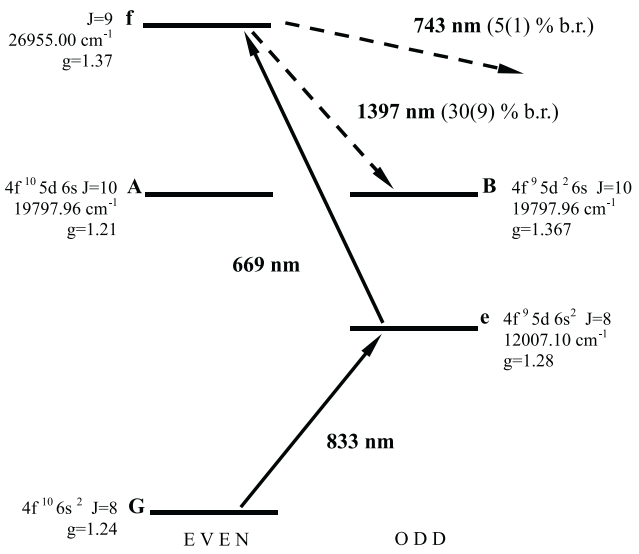

FIG. 2. Partial level diagram showing the transitions in the current population scheme. Solid arrows indicate excitation; dashed arrows indicate spontaneous decay.

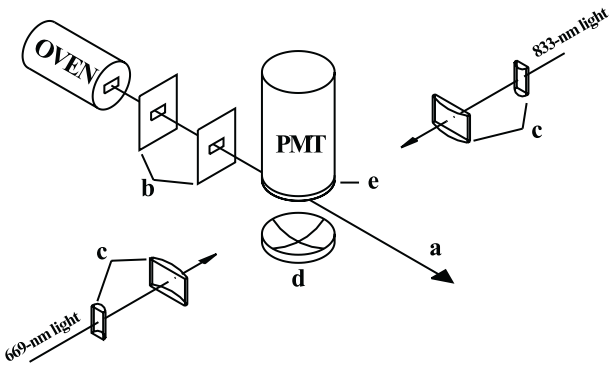

FIG. 3. Experimental setup (shown not to scale): a) atomic beam produced by an oven source at T=1500 K; b) atomic beam collimators; c) cylindrical lenses to diverge laser beams; d) spherical mirror to improve light collection efficiency; e) interference filter(s).

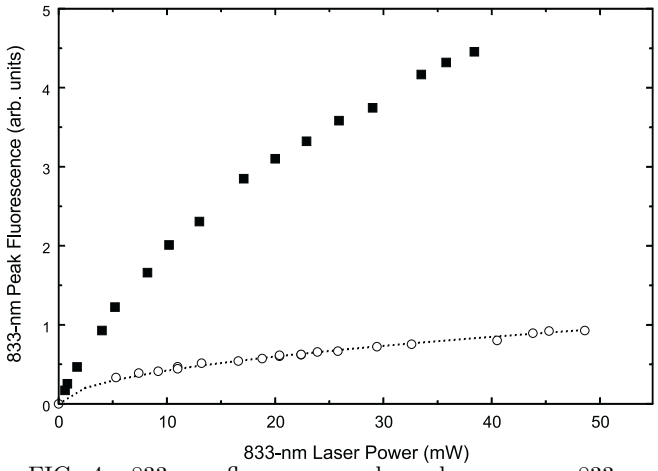

FIG. 4. 833-nm fluorescence dependence upon 833-nm laser power. The laser is tuned to resonance. Circles: zero beam divergence (without lenses); squares: a beam divergence of .06 rad (FWHM). Dotted curve: fit to a function of the form given in Eq. (5)

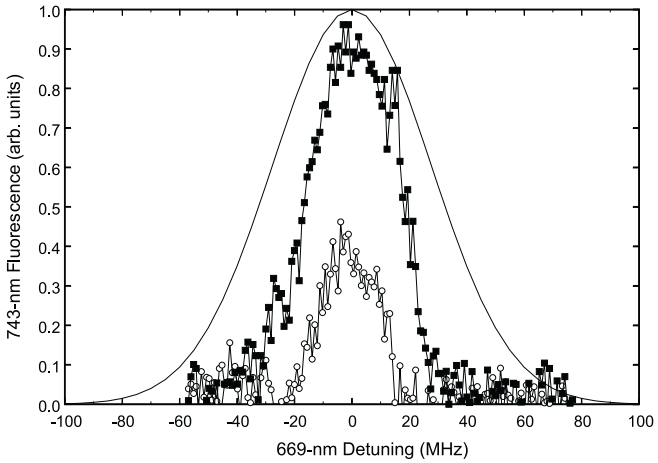

FIG. 5. 743-nm fluorescence curves obtained w/o lenses (circles) and w/ lenses (squares) in the 833-nm beam. The divergence was .05 rad (FWHM). Solid curve: transverse Doppler distribution of atoms.

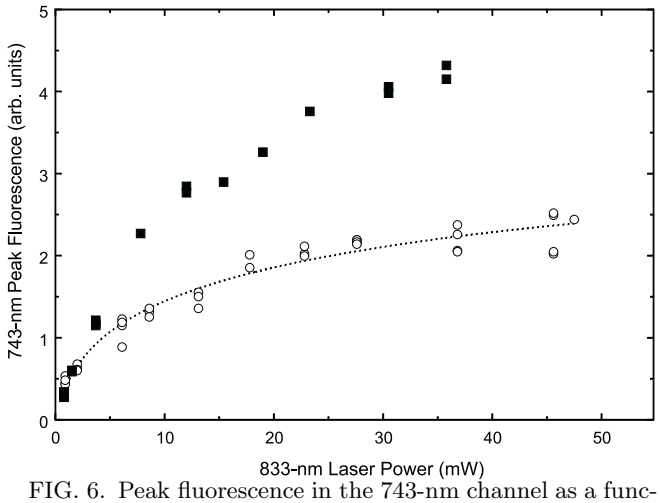

FIG. 6. Peak fluorescence in the 743-nm channel as a function of 833-nm laser power for the case w/o (circles) and w/ (squares) divergence in the 833-nm laser beam. Fluorescence is observed by probing with a low-power ($\approx$ 5mW, $\kappa_0 = .5$) 669-nm beam. For the case w/ lenses, the 833-nm laser divergence is .10 rad (FWHM). The dotted curve is a fit to a function of the form given by Eq. (1)

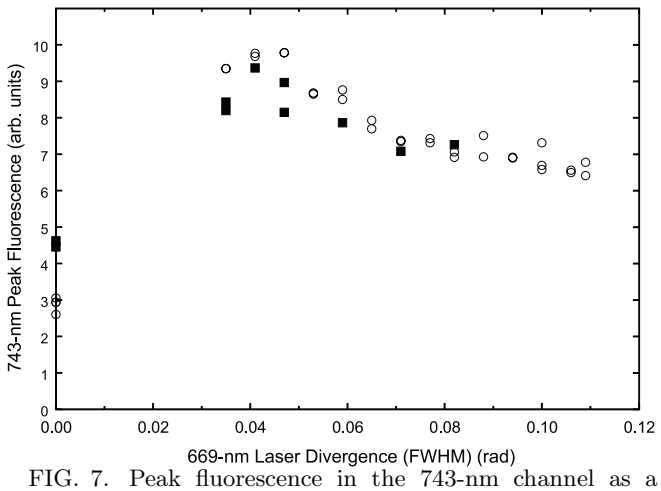

FIG. 7. Peak fluorescence in the 743-nm channel as a function of 669-nm laser divergence. 833-nm laser beam divergences are .06 rad (FWHM) (circles) and .04 rad (FWHM)(squares).